Final Paper for MAT4996: Modelling the Impact of a Live Virus Vaccine for Tularemia

Authors: K. Addison, K. Gee

Date submtted: April 17 2011

Contents

1 Introduction

Tularemia is an infectious disease caused by the bacteria *Francisella tularensis*. Typically found in North America, Europe and Asia, the spread and incidence of the disease has been steadily decreasing in recent years [5]. Tularemia occurs primarily in the Northern Hemisphere, with regular incidence of disease in Czech Republic, Finland, Japan, Kazakhstan, Slovakia, Sweden, Russia, US and Uzbekistan [2]. In particular, tularemia cases in the US are mainly concentrated in Arkansas, Missouri and Oklahoma, which account for 42.45% of all cases from 2000-2008 [21]. Nowadays, the prevalence and incidence of tularemia is fairly low, though it is endemic in certain rural regions and numerous small outbreaks have been reported in recent decades.

Several animals and arthropods can carry the disease and the disease itself naturally occurs in the wild. In particular, ticks, deer flies, horse flies and mosquitoes are known to contribute significantly to the transmission of the disease [20]. The animal population can contract the disease due to interaction with infected arthropods or with the contaminated environment. As environmental factors and arthropods are wide ranging, the disease has been noted in domestic animals, wild small mammals and fish [4]. While human to human transmission has not yet been reported, humans can contract tularemia through a number of different methods, including [5]:

– Fly and tick bites spreading the disease from animals to humans
– Contact with infected animals, including consumption of infected meat
– Drinking contaminated water or inhalation of infected particles

Tularemia in humans can manifest in several different forms: ulceroglandular, oculoglandular, pneumonic, oropharyngeal, gastrointestinal and typhoidal [4]. The most common form is ulceroglandular, which accounts for 80% of cases and has a fatality rate of 5% in untreated cases [4]. If tularemia has been ingested through contaminated meat or infected water, then it will likely display itself as either oropharyngeal or gastrointestinal tularemia [4]. Cases of oropharyngeal and gastrointestinal tularemia have the highest untreated fatality rate of any manifestation with 60%. Contact with airborne tularemia with the eyes may lead to oculoglandular or pneumonic tularemia, the latter of which has an untreated fatality rate of 40% [4].

Current methods of prevention for the general public are limited to techniques that reduce their exposure to infected animals and ticks [5]. Once infected, there is an effective antibiotic regimen that limits the mortality rate to below 2% [5]. Recovery for most individuals results in long-lasting immunity to the disease [5]. As the bacteria are highly infective and easy to aerosolize, the disease has been recognized as a potential bioterrorism weapon. This has led to increased interest in the development and production of vaccines [7]. Current vaccines include an attenuated form of the

Francisella tularensis live vaccine strain (LVS), which has been available for several decades. This vaccine, while efficacious against non-aerosol forms of transmission, offers less protection against aerosol transmission. Furthermore, as the basis for the immune response and rate of reversion are unknown, it has not been deemed safe enough to distribute to the general public and has only been distributed to individuals of high risk who are in constant contact with the disease [2,7].

Most studies of tularemia to date have been clinical in nature. Past studies have addressed the disease, vaccine and drug options [2, 4, 5], as well as transmission and infection sources during an outbreak [8]. Studies have also focused on the clinical diagnosis of tularemia [9], and verifying the efficacy of the live vaccine [6]. Mathematical modeling of this disease has received relatively little attention.

This paper will attempt to model tularemia within a small group of organisms. It will also examine how a live vaccine for the susceptible human population can control the infected human population in the long run, despite the presence of an animal reservoir. While we will provide numerical simulations using estimates of the parameters, the lack of reliable data makes it difficult to realistically predict how the system will evolve over time.

2 The Mathematical Model using Ordinary Differential Equations

We will first consider the model without vaccination to examine various dynamics of the system before extending the model to include impulsive vaccinations occuring at regular intervals. Numerical simulations of the system will then illustrate the effect of the vaccine.

2.1 System without vaccination

For the basic model of tularemia, we consider eight populations. Contamination of the environment, in the form of infected airborne particles or contaminated water, will be treated as a population in order to consider its effects on the dynamics of the other three populations:

Populations	
S_I	Susceptible insect population
I_I	Infectious insect population
S_A	Susceptible animal population
I_A	Infectious animal population
S_H	Susceptible human population
I_H	Infectious human population
R_H	Recovered human population
E	Contaminated environment

By using a system of ordinary differential equations to characterize the system, we assume that the populations are large and mix homogeneously so that we can treat them as a continuous function of time. This is considered to be valid for the population of animals, insects and the environment, as they are in constant contact with each other. This may also hold for the human population when considering an isolated rural village.

For this model, we assume that there is constant birth rates within the insect, animal and human populations (π_I, π_A, π_H), and that all offspring are born susceptible to the disease. There is also constant background death or decay rates within the insect, animal, human and environment populations (μ_I, μ_A, μ_H, μ_E).

Susceptible individuals become infected through mass-action transmission after interaction with infected organisms in the other populations (α_i, for i = 1 to 7) and subsequently move into their respective infected populations. Susceptible animals can become infected through exposure to the contaminated environment (ρ_1), and susceptible humans can become infected through exposure to contaminated water (ρ_2) and air (ρ_3). Infected animals and humans can recover from the

disease (β_A, β_H), though only humans recover with lifelong immunity. Finally, infected animals and humans can die at a disease-specific death rate that is higher than the background death rate (γ_A, γ_H).

These interactions produce the following ODE model:

$$
\begin{aligned}
S_I' &= \pi_I - \alpha_2 I_A S_I - \alpha_6 I_H S_I - \mu_I S_I \\
I_I' &= \alpha_2 I_A S_I + \alpha_6 I_H S_I - \mu_I I_I \\
S_A' &= \pi_A - \alpha_1 I_I S_A - \alpha_3 I_A S_A - \rho_1 E S_A + \beta_A I_A - \mu_A S_A \\
I_A' &= \alpha_1 I_I S_A + \alpha_3 I_A S_A + \rho_1 E S_A - \beta_A I_A - \gamma_A I_A - \mu_A I_A \\
S_H' &= \pi_H - \alpha_4 I_A S_H - \alpha_5 I_I S_H - (\rho_2 + \rho_3) E S_H - \mu_H S_H \\
I_H' &= \alpha_4 I_A S_H + \alpha_5 I_I S_H + (\rho_2 + \rho_3) E S_H - \beta_H I_H - \gamma_H I_H - \mu_H I_H \\
R_H' &= \beta_H I_H - \mu_H R_H \\
E' &= \alpha_7 I_A - \mu_E E
\end{aligned}
\tag{1}
$$

where the population is at time $t = 0$ and all of the parameters are positive.

The interactions between the different populations are illustrated in Figure 1 below:

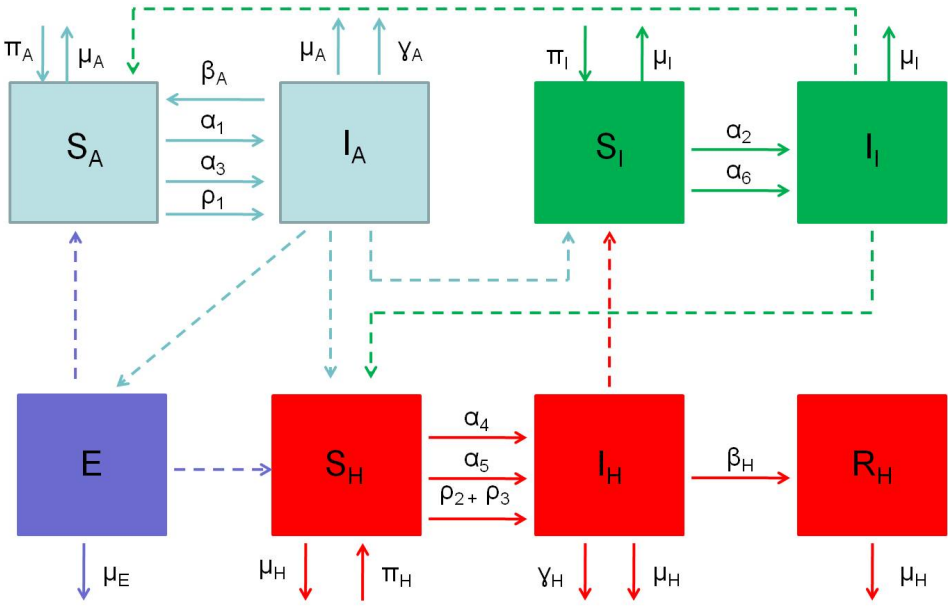

Figure 1: *Flowchart of the model without vaccination. The dashed lines represent routes of transmission, while the solid lines represent transfer of individuals from one compartment to another.*

Using model (1), the disease-free equilibrium population values are:

$\{S_I^*, I_I^*, S_A^*, I_A^*, S_H^*, I_H^*, R_H^*, E^*\} = \{\frac{\pi_I}{\mu_I}, 0, \frac{\pi_A}{\mu_A}, 0, \frac{\pi_H}{\mu_H}, 0, 0, 0\}$

Otherwise, the endemic equilibrium values are:

$$S_I^* = \frac{\mu_I I_I^*}{\alpha_2 I_A^* + \alpha_6 I^* H}$$

$$S_A^* = \frac{(\beta_A + \gamma_A + \mu_A) I_A^*}{\alpha_1 I_I^* + \alpha_3 I_A^* + \rho_1 \dfrac{\alpha_7 I_A^*}{\mu_E}}$$

$$S_H^* = \frac{\pi_H}{\alpha_4 I_A^* + \alpha_5 I_I^* + (\rho_2 + \rho_3)\dfrac{\alpha_7 I_A^*}{\mu_E} + \mu_H}$$

$$R_H^* = \frac{\beta_H I_H^*}{\mu_H}$$

$$E^* = \frac{\alpha_7 I_A^*}{\mu_E}$$

where $I_H^* = \left(\dfrac{\alpha_4 I_A^* + \alpha_5 I_I^* + (\rho_2 + \rho_3)\dfrac{\alpha_7 I_A^*}{\mu_E}}{\alpha_4 I_A^* + \alpha_5 I_I^* + (\rho_2 + \rho_3)\dfrac{\alpha_7 I_A^*}{\mu_E} + \mu_H} \right) \left(\dfrac{\pi_H}{\beta_H + \gamma_H + \mu_H} \right)$, and I_A^* and I_I^* are obtained by solving: $I_I^* = \dfrac{\pi_I(\alpha_2 I_A^* + \alpha_6 I_H^*)}{\mu_I(\alpha_2 I_A^* + \alpha_6 I_H^* + \mu_I)}$ and $\dfrac{\pi_A + \beta_A I_I^*}{\alpha_1 I_I^* + \alpha_3 I_A^* + \rho_1 \dfrac{\alpha_7 I_A^*}{\mu_E} + \mu_A} = \dfrac{\pi_A - I_A^*(\gamma_A + \mu_A)}{\mu_A}$ for given parameters.

Theorem 2.1.1. *Define*

$$A = \mu_I - \alpha_3 \frac{\pi_A}{\mu_A} + \beta_A + \gamma_A + \mu_A + \mu_E + \beta_H + \gamma_H + \mu_H$$

$$B = -\alpha_6 \alpha_5 \frac{\pi_I}{\mu_I} \frac{\pi_H}{\mu_H} + (\mu_E + \beta_H + \gamma_H + \mu_H) \left(\mu_I - \alpha_3 \frac{\pi_A}{\mu_A} + \beta_A + \gamma_A + \mu_A \right) + \mu_I \left(\beta_A + \gamma_A + \mu_A - \alpha_3 \frac{\pi_A}{\mu_A} \right) + \mu_E (\beta_H + \gamma_H + \mu_H) + \alpha_1 \alpha_2 \frac{\pi_A}{\mu_A} \frac{\pi_I}{\mu_I}$$

$$C = \alpha_6 \frac{\pi_I}{\mu_I} \frac{\pi_H}{\mu_H} \left(\alpha_5 (\alpha_3 \frac{\pi_A}{\mu_A} - \mu_E - \beta_A - \gamma_A - \mu_A) - \alpha_1 \alpha_4 \frac{\pi_A}{\mu_A} \right) + \mu_E (\beta_H + \gamma_H + \mu_H) \left(\mu_I - \alpha_3 \frac{\pi_A}{\mu_A} + \beta_A + \gamma_A + \mu_A \right) + \mu_I \left(\beta_A + \gamma_A + \mu_A - \alpha_3 \frac{\pi_A}{\mu_A} \right) (\beta_H + \gamma_H + \mu_H + \mu_E) - \rho_1 \alpha_7 \frac{\pi_A}{\mu_A} (\mu_I + \beta_H + \gamma_H + \mu_H)$$

$$D = \alpha_6 \frac{\pi_I}{\mu_I} \frac{\pi_H}{\mu_H} \left(\alpha_5 \mu_E \left(\alpha_3 \frac{\pi_A}{\mu_A} - \beta_A - \gamma_A - \mu_A \right) + \rho_1 \alpha_5 \alpha_7 \frac{\pi_A}{\mu_A} - \alpha_1 \frac{\pi_A}{\mu_A} (\alpha_4 \mu_E + \alpha_7 (\rho_2 + \rho_3)) \right) + \mu_E (\beta_H + \gamma_H + \mu_H) \left(\mu_I \left(\beta_A + \gamma_A + \mu_A - \alpha_3 \frac{\pi_A}{\mu_A} \right) - \alpha_1 \alpha_2 \frac{\pi_A}{\mu_A} \frac{\pi_I}{\mu_I} \right) - \rho_1 \alpha_7 \mu_I \frac{\pi_A}{\mu_A} (\beta_H + \mu_H + \gamma_H)$$

If $h_0 = min\{A, D, AB - C, C(AB - C) - A^2D\} > 0$*, the disease-free equilibrium is stable. Otherwise, the disease-free equilibrium is unstable.*

Proof. It suffices to provide the conditions in which all of the eigenvalues of the Jacobian matrix of Model (1) when evaluated at the DFE have a negative real part. The Jacobian matrix for model (1) is $J = [J1|J2]$ where J1 and J2 are as follows:

$$J_1 = \begin{bmatrix} -\alpha_2 I_A - \alpha_6 I_H - \mu_I & 0 & 0 & -\alpha_2 S_I \\ \alpha_2 I_A + \alpha_6 I_H & -\mu_I & 0 & \alpha_2 S_I \\ 0 & -\alpha_1 S_A & -\alpha_1 I_I - \alpha_3 I_A - \rho_1 E - \mu_A & -\alpha_3 S_A + \beta_A \\ 0 & \alpha_1 S_A & \alpha_1 I_I + \alpha_3 I_A + \rho_1 E & \alpha_3 S_A - \beta_A - \gamma_A - \mu_A \\ 0 & -\alpha_5 S_H & 0 & -\alpha_4 S_H \\ 0 & \alpha_5 S_H & 0 & \alpha_4 S_H \\ 0 & 0 & 0 & 0 \\ 0 & 0 & 0 & \alpha_7 \end{bmatrix}$$

$$J_2 = \begin{bmatrix} 0 & -\alpha_6 S_I & 0 & 0 \\ 0 & \alpha_6 S_I & 0 & 0 \\ 0 & 0 & 0 & -\rho_1 S_A \\ 0 & 0 & 0 & \rho_1 S_A \\ -\alpha_4 I_A - \alpha_5 I_I - \rho_2 E - \rho_3 E - \mu_H & 0 & 0 & -\rho_2 S_H - \rho_3 S_H \\ \alpha_4 I_A + \alpha_5 I_I + \rho_2 E + \rho_3 E & -\beta_H - \gamma_H - \mu_H & 0 & \rho_2 S_H + \rho_3 S_H \\ 0 & \beta_H & -\mu_H & 0 \\ 0 & 0 & 0 & -\mu_E S \end{bmatrix}$$

When evaluated at the disease-free equilibrium, $J = J_0$ which is equal to the following:

$$J_0 = \begin{bmatrix} -\mu_I & 0 & 0 & -\alpha_2 \frac{\pi_I}{\mu_I} & 0 & -\alpha_6 \frac{\pi_I}{\mu_I} & 0 & 0 \\ 0 & -\mu_I & 0 & \alpha_2 \frac{\pi_I}{\mu_I} & 0 & \alpha_6 \frac{\pi_I}{\mu_I} & 0 & 0 \\ 0 & -\alpha_1 \frac{\pi_A}{\mu_A} & -\mu_A & -\alpha_3 \frac{\pi_A}{\mu_A} + \beta_A & 0 & 0 & 0 & -\rho_1 \frac{\pi_A}{\mu_A} \\ 0 & \alpha_1 \frac{\pi_A}{\mu_A} & 0 & \alpha_3 \frac{\pi_A}{\mu_A} - \beta_A - \gamma_A - \mu_A & 0 & 0 & 0 & \rho_1 \frac{\pi_A}{\mu_A} \\ 0 & -\alpha_5 \frac{\pi_H}{\mu_H} & 0 & -\alpha_4 \frac{\pi_H}{\mu_H} & -\mu_H & 0 & 0 & -\rho_2 \frac{\pi_H}{\mu_H} - \rho_3 \frac{\pi_H}{\mu_H} \\ 0 & \alpha_5 \frac{\pi_H}{\mu_H} & 0 & \alpha_4 \frac{\pi_H}{\mu_H} & 0 & -\beta_H - \gamma_H - \mu_H & 0 & \rho_2 \frac{\pi_H}{\mu_H} + \rho_3 \frac{\pi_H}{\mu_H} \\ 0 & 0 & 0 & 0 & 0 & \beta_H & -\mu_H & 0 \\ 0 & 0 & 0 & \alpha_7 & 0 & 0 & 0 & -\mu_E \end{bmatrix}$$

The eigenvalues satisfy the roots of the characteristic equation:

$$0 = (-\mu_H - \lambda)^2(-\mu_A - \lambda)(-\mu_I - \lambda) \det \begin{vmatrix} -\mu_I - \lambda & \alpha_2 \frac{\pi_I}{\mu_I} & \alpha_6 \frac{\pi_I}{\mu_I} & 0 \\ \alpha_1 \frac{\pi_A}{\mu_A} & \alpha_3 \frac{\pi_A}{\mu_A} - \beta_A - \gamma_A - \mu_A - \lambda & 0 & \rho_1 \frac{\pi_A}{\mu_A} \\ \alpha_5 \frac{\pi_H}{\mu_H} & \alpha_4 \frac{\pi_H}{\mu_H} & -\beta_H - \gamma_H - \mu_H - \lambda & \rho_2 \frac{\pi_H}{\mu_H} + \rho_3 \frac{\pi_H}{\mu_H} \\ 0 & \alpha_7 & 0 & -\mu_E - \lambda \end{vmatrix}$$

By assumption, μ_I, μ_A and μ_H are all strictly positive, so it suffices to examine the determinant of the matrix. This is a quartic of the form $\lambda^4 + A\lambda^3 + B\lambda^2 + C\lambda + D$, where A, B, C and D are equal to the following:

$$\begin{aligned}
A &= \mu_I - \alpha_3 \frac{\pi_A}{\mu_A} + \beta_A + \gamma_A + \mu_A + \mu_E + \beta_H + \gamma_H + \mu_H \\
B &= -\alpha_6 \alpha_5 \frac{\pi_I}{\mu_I} \frac{\pi_H}{\mu_H} + (\mu_E + \beta_H + \gamma_H + \mu_H) \left(\mu_I - \alpha_3 \frac{\pi_A}{\mu_A} + \beta_A + \gamma_A + \mu_A \right) + \mu_I \left(\beta_A + \gamma_A + \mu_A - \alpha_3 \frac{\pi_A}{\mu_A} \right) \\
&\quad + \mu_E (\beta_H + \gamma_H + \mu_H) + \alpha_1 \alpha_2 \frac{\pi_A}{\mu_A} \frac{\pi_I}{\mu_I} \\
C &= \alpha_6 \frac{\pi_I}{\mu_I} \frac{\pi_H}{\mu_H} \left(\alpha_5 (\alpha_3 \frac{\pi_A}{\mu_A} - \mu_E - \beta_A - \gamma_A - \mu_A) - \alpha_1 \alpha_4 \frac{\pi_A}{\mu_A} \right) + \mu_E (\beta_H + \gamma_H + \mu_H) \left(\mu_I - \alpha_3 \frac{\pi_A}{\mu_A} + \beta_A + \gamma_A + \mu_A \right) \\
&\quad + \mu_I \left(\beta_A + \gamma_A + \mu_A - \alpha_3 \frac{\pi_A}{\mu_A} \right) (\beta_H + \gamma_H + \mu_H + \mu_E) - \rho_1 \alpha_7 \frac{\pi_A}{\mu_A} (\mu_I + \beta_H + \gamma_H + \mu_H) \\
D &= \alpha_6 \frac{\pi_I}{\mu_I} \frac{\pi_H}{\mu_H} \left(\alpha_5 \mu_E \left(\alpha_3 \frac{\pi_A}{\mu_A} - \beta_A - \gamma_A - \mu_A \right) + \rho_1 \alpha_5 \alpha_7 \frac{\pi_A}{\mu_A} - \alpha_1 \frac{\pi_A}{\mu_A} (\alpha_4 \mu_E + \alpha_7 (\rho_2 + \rho_3)) \right) \\
&\quad + \mu_E (\beta_H + \gamma_H + \mu_H) \left(\mu_I \left(\beta_A + \gamma_A + \mu_A - \alpha_3 \frac{\pi_A}{\mu_A} \right) - \alpha_1 \alpha_2 \frac{\pi_A}{\mu_A} \frac{\pi_I}{\mu_I} \right) - \rho_1 \alpha_7 \mu_I \frac{\pi_A}{\mu_A} (\beta_H + \mu_H + \gamma_H)
\end{aligned}$$

According to the Routh-Hurwitz stability criterion, all of the roots will have a negative part if $A > 0$, $D > 0$, $AB - C > 0$, and $C(AB - C) > A^2 D$, which provides us with the conditions outlined in the theorem.

□

Note that the criteria $A > 0$ is unlikely to hold if $\alpha_3 > 0$, as $\alpha_3 \frac{\pi_A}{\mu_A}$ is likely much larger than $\mu_I + \beta_A + \gamma_A + \mu_A + \mu_E + \beta_H + \gamma_H + \mu_H$, in which case $A = \mu_I - \alpha_3 \frac{\pi_A}{\mu_A} + \beta_A + \gamma_A + \mu_A + \mu_E + \beta_H + \gamma_H + \mu_H < 0$.

2.2 System with Vaccination

We will now turn our attention to the system with pulse vaccinations at regular time intervals (τ) to a proportion of the susceptible human population (p). This vaccine has different efficacies for aerosol transmission (θ_2) and for the other methods of transmission (θ_1), and also reverts to the original viral strain at a given rate (ϕ). This system, in ODE form, is illustrated below.

For $t \neq t_k$:

$$\begin{aligned}
S_I' &= \pi_I - \alpha_2 I_A S_I - \alpha_6 I_H S_I - \mu_I S_I \\
I_I' &= \alpha_2 I_A S_I + \alpha_6 I_H S_I - \mu_I I_I \\
S_A' &= \pi_A - \alpha_1 I_I S_A - \alpha_3 I_A S_A - \rho_1 E S_A + \beta_A I_A - \mu_A S_A \\
I_A' &= \alpha_1 I_I S_A + \alpha_3 I_A S_A + \rho_1 E S_A - \beta_A I_A - \gamma_A I_A - \mu_A I_A \\
S_H' &= \pi_H - \alpha_4 I_A S_H - \alpha_5 I_I S_H - (\rho_2 + \rho_3) E S_H - \mu_H S_H \\
I_H' &= \alpha_4 I_A S_H + \alpha_5 I_I S_H + \rho_2 E S_H + \rho_3 E S_H + (1-\theta_1)(\alpha_4 I_A V_H + \alpha_5 I_I V_H + \rho_2 E V_H) + \\
&\quad (1-\theta_2)\rho_3 E V_H + \phi V_H - \beta_H I_H - \gamma_H I_H - \mu_H I_H \\
R_H' &= \beta_H I_H - \mu_H R_H \\
E' &= \alpha_7 I_A - \mu_E E \\
V_H' &= -(1-\theta_1)(\alpha_4 I_A V_H + \alpha_5 I_I V_H + \rho_2 E V_H) - (1-\theta_2)\rho_3 E V_H - \phi V_H - \mu_H V_H
\end{aligned} \tag{2}$$

The impulsive conditions are given by:

$$\begin{aligned}
\Delta S_H &= -p S_H^- \\
\Delta V_H &= p S_H^-
\end{aligned} \tag{3}$$

for $t = t_k$.

The inherent assumption in adding an impulsive component to the model is that the changes happen instantaneously, which is a relatively safe assumption if enough clinics are set up so that all of the vaccinations can occur within a day. Due to the impulsive effects, the populations do not reach an equilibrium. However, we may attempt to find impulsive orbits for these populations and arrive at a bound for the infected human population as $t \to \infty$.

For notational purses, define $c_1 \equiv \alpha_4 I_A^* + \alpha_5 I_I^* + \rho_2 E^* + \rho_3 E^* + \mu_H$
and $c_2 \equiv (1-\theta_1)(\alpha_4 I_A^* + \alpha_5 I_I^* + \rho_2 E^*) + (1-\theta_2)\rho_3 E^* + \phi + \mu_H$, where I_A^*, I_I^*, E^* are the equilibrium values of the populations in the model without vaccination.

Theorem 2.2.1. *Let $X(t_k^-)$ denote the k^{th} endpoint immediately before the impulse. Then*

$$S_H^*(t_k^-) = \frac{\pi_H}{c_1}\left(1 - \frac{pe^{-c_1\tau}}{1-(1-p)e^{-c_1\tau}}\right)$$

and

$$V_H^*(t_k^-) = \frac{pe^{-c_2\tau}}{1-e^{-c_2\tau}} S_H^*(t_k^-)$$

are globally asymptotically stable fixed points for the endpoint before the impulse for S_H and V_H.

Proof. First consider the susceptible human population. Let $f_1(t) \equiv \alpha_4 I_A(t) + \alpha_5 I_I(t) + \rho_2 E(t) + \rho_3 E(t) + \mu_H$. Then, from Model (2):

$S' = \pi_H - \alpha_4 I_A S_H - \alpha_5 I_I S_H - \rho_2 E S_H - \rho_3 E S_H - \mu_H S_H = \pi_H - f_1(t) S_H(t)$, which implies that

$$\frac{d}{dt}\left(S_H e^{\int f_1(s)\,ds}\right) = \pi_H e^{\int f_1(s)\,ds}.$$

Then it follows that for $t_k < t \leq t_{k+1}$:

$$S_H(t) = \frac{1}{e^{\int f_1(s)\,ds}\Big|_{s=t}}\left[S_H(t_k^+)e^{\int f_1(s)\,ds}\Big|_{s=t_k} + \int_{t_k}^{t} \pi_H e^{\int f_1(s)\,ds} ds\right]$$

and after factoring in the impulsive effect and setting $t = t_{k+1}$,

$$S_H(t_{k+1}^-) = \frac{1}{e^{\int f_1(s)\,ds}\Big|_{s=t_{k+1}}}\left[(1-p)S_H(t_k^-)e^{\int f_1(s)\,ds}\Big|_{s=t_k} + \int_{t_k}^{t_{k+1}} \pi_H e^{\int f_1(s)\,ds} ds\right]$$

Let $S_H(t_0) = \frac{1}{1-p} S_H(0)$ where $S_H(0)$ is the initial population of S_H. Then

$$S_H(t_1^-) = \frac{1}{e^{\int f_1(s)\,ds}\Big|_{s=t_1}}\left[(1-p)S_H(t_0)e^{\int f_1(s)\,ds}\Big|_{s=t_0} + \int_{t_0}^{t_1} \pi_H e^{\int f_1(s)\,ds} ds\right]$$

$$S_H(t_2^-) = \frac{1}{e^{\int f_1(s)\,ds}\Big|_{s=t_2}}\left[(1-p)\left[(1-p)S_H(t_0)e^{\int f_1(s)\,ds}\Big|_{s=t_0} + \int_{t_0}^{t_1} \pi_H e^{\int f_1(s)\,ds} ds\right] + \int_{t_1}^{t_2} \pi_H e^{\int f_1(s)\,ds} ds\right]$$

...

$$S_H(t_k^-) = \frac{1}{e^{\int f_1(s)\,ds}\Big|_{s=t_k}} \left[(1-p)^k S_H(t_0) e^{\int f_1(s)\,ds}\Big|_{s=t_0} + \sum_{j=0}^{k-1} (1-p)^j \int_{t_{k-j-1}}^{t_{k-j}} \pi_H e^{\int f_1(s)\,ds} ds \right]$$

Let w be the smallest integer such that for $t \geq t_w$, I_I, I_A and E are all approximately at their equilibrium values. We will now make the assumption that the equilibrium values for these populations are the same as in the model without vaccination and moreover, are constant. This assumption was made because the infected populations are dependent upon multiple populations, of which only a couple are directly affected by the impulses. Furthermore, as seen in Figure 3 in Section 2.3, this assumption is fairly accurate. Then for $t \geq t_w$, $f_1(t) \approx \alpha_4 I_A^* + \alpha_5 I_I^* + \rho_2 E^* + \rho_3 E^* + \mu_H = c_1$ and so, for $k \geq w$:

$$\begin{aligned}
S_H(t_k^-) &\approx \frac{(1-p)^k S_H(t_0) e^{\int f_1(s)\,ds}\Big|_{s=t_0}}{e^{c_1 t_k}} + \sum_{j=0}^{w-1} \frac{\pi_H (1-p)^{k-w+j} \int_{t_{w-j-1}}^{t_{w-j}} e^{\int f_1(s)\,ds} ds}{e^{c_1 t_k}} + \sum_{j=0}^{k-w-1} \frac{\pi_H (1-p)^j}{c_1} \left(\frac{e^{c_1 t_{k-j}} - e^{c_1 t_{k-j-1}}}{e^{c_1 t_k}} \right) \\
&= \frac{(1-p)^k S_H(t_0) e^{\int f_1(s)\,ds}\Big|_{s=t_0}}{e^{c_1 t_k}} + \pi_H (1-p)^{k-w} \sum_{j=0}^{w-1} \frac{(1-p)^j \int_{t_{w-j-1}}^{t_{w-j}} e^{\int f_1(s)\,ds} ds}{e^{c_1 t_k}} \\
&+ \sum_{j=0}^{k-w-1} \frac{\pi_H (1-p)^j}{c_1} \left(e^{-c_1(t_k - t_{k-j})} - e^{-c_1(t_k - t_{k-j-1})} \right) \\
&= \frac{(1-p)^k S_H(t_0) e^{\int f_1(s)\,ds}\Big|_{s=t_0}}{e^{c_1 t_k}} + \pi_H (1-p)^{k-w} \sum_{j=0}^{w-1} \frac{(1-p)^j \int_{t_{w-j-1}}^{t_{w-j}} e^{\int f_1(s)\,ds} ds}{e^{c_1 t_k}} + \sum_{j=0}^{k-w-1} \frac{\pi_H (1-p)^j e^{-c_1 j\tau}}{c_1} \left(1 - e^{-c_1\tau}\right) \\
&= \frac{(1-p)^k S_H(t_0) e^{\int f_1(s)\,ds}\Big|_{s=t_0}}{e^{c_1 t_k}} + \pi_H (1-p)^{k-w} \sum_{j=0}^{w-1} \frac{(1-p)^j \int_{t_{w-j-1}}^{t_{w-j}} e^{\int f_1(s)\,ds} ds}{e^{c_1 t_k}} + \frac{\pi_H (1 - e^{-c_1\tau})}{c_1} \left(\frac{1 - (1-p)^{k-w} e^{-c_1\tau(k-w)}}{1 - (1-p)e^{-c_1\tau}} \right)
\end{aligned}$$

As $k \to \infty$, $(1-p)^k \to 0$, $(1-p)^{k-w} \to 0$ and $e^{-c_1\tau(k-w)} \to 0$ and so,:

$$\begin{aligned}
S_H^*(t_k^-) &\to \frac{\pi_H (1 - e^{-c_1\tau})}{c_1} \left(\frac{1}{1 - (1-p)e^{-c_1\tau}} \right) \\
&= \frac{\pi_H}{c_1} \left(1 - \frac{p e^{-c_1\tau}}{1 - (1-p)e^{-c_1\tau}} \right)
\end{aligned}$$

We apply a similar treatment to the vaccinated human population:

Let $f_2(t) \equiv (1-\theta_1)(\alpha_4 I_A + \alpha_5 I_I V_H + \rho_2 E V_H) + (1-\theta_2)\rho_3 E V_H + \phi V_H + \mu_H V_H$. From Model (2), $V' = -(1-\theta_1)(\alpha_4 I_A V_H + \alpha_5 I_I V_H + \rho_2 E V_H) - (1-\theta_2)\rho_3 E V_H - \phi V_H - \mu_H V_H = -f_2 V_H$ and so,

$\frac{dV_H}{dt}\frac{1}{V_H} = -f_2(t)$ or for $t_k < t \leq t_{k+1}$, $V_H(t) = V_H(t_k^+)e^{-\int_{t_k}^{t} f_2(s)ds}$. After accounting for the impulsive effects and setting $t = t_{k+1}$:

$V_H(t_{k+1}^-) = \left(V_H(t_k^-) + pS_H(t_k^-)\right) e^{-\int_{t_k}^{t_k+1} f_2(s)ds}$. Then, if $V_H(t_0) = V_H(0) - pS_H(t_0)$:

$V_H(t_1^-) = \left(V_H(t_0) + pS_H(t_0)\right) e^{-\int_{t_0}^{t_1} f_2(s)ds}$
$V_H(t_2^-) = \left[\left(V_H(t_0) + pS_H(t_0)\right) e^{-\int_{t_0}^{t_1} f_2(s)ds} + pS_H(t_1^-)\right] e^{-\int_{t_1}^{t_2} f_2(s)ds}$

...

$V_H(t_k^-) = V_H(t_0)\prod_{l=1}^{k} e^{-\int_{t_{k-l}}^{t_{k-l+1}} f_2(s)ds} + \sum_{j=0}^{k-1} pS_H(t_j^-)\prod_{l=1}^{k-j} e^{-\int_{t_{k-l}}^{t_{k-l+1}} f_2(s)ds}$

For $t \geq t_w$, $f_2(t) \approx (1-\theta_1)(\alpha_4 I_A^* + \alpha_5 I_I^* + \rho_2 E^*) + (1-\theta_2)\rho_3 E^* + \phi + \mu_H = c_2$ and so, as $k \to \infty$, then $V_H(t_0)\prod_{l=1}^{k} e^{-\int_{t_{k-l}}^{t_{k-l+1}} f_2(s)ds} \to 0$. Furthermore, as seen above, for given values of I_A^*, I_I^*, E^*, $S_H(t_k^-)$ converges to a single fixed point and so, $V_H(t_k^-)$ will also converge to a single fixed point. It remains to find this fixed point, which will occur where

$$\begin{aligned} V_H(t_k^-) &= V_H(t_{k+1}^-) \\ &= \left(V_H(t_k^-) + pS_H^*(t_k^-)\right) e^{-c_2\tau} \end{aligned}$$

which implies that $V_H^*(t_k^-) = \frac{pe^{-c_2\tau}}{1-e^{-c_2\tau}} S_H^*(t_k^-)$.

□

Using these endpoints, we can make inferences about the infected human population, which is our population of interest. This analysis will use the following lemma:

Lemma 2.2.1. *If $X' \leq k - lX(t)$ for constants $k > 0$ and $l > 0$, then $X(t)$ will converge to a value that is less than or equal to $\frac{k}{l}$.*

Furthermore, if $X' \geq k - lX(t)$, then $X(t)$ will converge to a value that is larger than or equal to $\frac{k}{l}$.

Proof. Given that $\frac{dX(t)}{dt} \leq k - lX(t)$, this implies that $\frac{dX(t)}{dt} + lX(t) \leq k$ or $\frac{d}{dt}X(t)e^{lt} \leq ke^{lt}$.

Therefore, $X(t) \leq X(0)e^{-lt} + \frac{k}{l}(1-e^{-lt})$. As t $\to \infty$, $e^{-lt} \to 0$ and so, $X(t)$ will converge to a

value that is less than $\frac{k}{l}$.

The second part of the theorem follows by reversing the inequalities above.

□

This will be used to help prove that with appropriate vaccination parameters, we can reduce the infected human population below any given threshold as $t \to \infty$.

Theorem 2.2.2. *Let I_A^*, I_I^*, E^* be the equilibrium values of I_A, I_I and E respectively in the model without vaccination. Then $I_H(t)$ can be reduced below any threshold as $t \to \infty$ with appropriate p, τ, θ_1, θ_2, and ϕ.*

Proof. Let $\epsilon > 0$ denote the desired threshold of infected humans and I_A^*, I_I^* and E^* be the equilibrium values of I_A, I_I and E respectively in the model without vaccination. Furthermore, note that by Model (2),

$I'_H = S_H(f_1 - \mu_H) + (1-\theta_1)(\alpha_4 I_A V_H + \alpha_5 I_I V_H + \rho_2 E V_H) + (1-\theta_2)\rho_3 E V_H + \phi V_H - \beta_H I_H - \gamma_H I_H - \mu_H I_H$
where $f_3(t) = \alpha_4 I_A(t) + \alpha_5 I_I(t) + \rho_2 E(t) + \rho_3 E(t) - \mu_H$.

Then let w be the smallest integer such that for $t \geq t_w$, I_I, I_A and E all attain their equilibrium values and $S_H(t_w^-)$ and $V_H(t_w^-)$ are both at their impulsive orbits. Similar to our previous analysis, we will assume that the population equilibrium values are approximately the same as in the model without vaccination so that we can treat it as a constant and $f_1 \approx c_1$. Therefore, consider $t \geq t_w$.

As S_H has attained its impulsive periodic orbit, it follows that as $S'_H > 0$ for $t_k < t \leq t_{k+1}$, then for all $t \geq t_w$, $S_H(t) \leq S_H^*(t_k^-) = \frac{\pi_H}{c_1}\left(1 - \frac{pe^{-c_1\tau}}{1-(1-p)e^{-c_1\tau}}\right)$. This can be made arbitrarily small for p close to 1 and τ close to 0. Therefore, choose an appropriate p and τ such that $S_H^*(t_k^-) \leq \frac{\epsilon(\beta_H + \mu_H + \gamma_H)}{4(c_1 - \mu_H)}$.

Furthermore, as V_H is also at its impulsive orbit, note that $V'_H < 0$ for $t_k < t \leq t_{k+1}$ or that for all $t \geq t_w$, $V_H(t) \leq V_H^*(t_k^+) = V_H^*(t_k^-) + pS_H^*(t_k^-) = \frac{pe^{-c_2\tau}}{1-e^{-c_2\tau}} S_H^*(t_k^-) + pS_H^*(t_k^-) = S_H^*(t_k^-)\frac{p}{1-e^{-c_2\tau}}$. This is well-defined for the values of p and τ chosen above. Therefore, we can choose θ_1 such that

$(1-\theta_1) \leq \frac{\epsilon(\beta_H + \mu_H + \gamma_H)}{4V_H^*(t_k^+)(\alpha_4 I_A^* + \alpha_5 I_I^* + \rho_2 E^*)}$.

Similarly, choose θ_2 such that $(1-\theta_2) \leq \frac{\epsilon(\beta_H + \mu_H + \gamma_H)}{4V_H^*(t_k^+)\rho_3 E^*}$.

Finally, choose ϕ such that $\phi \leq \frac{\epsilon(\beta_H + \mu_H + \gamma_H)}{4V_H^*(t_k^+)}$.

Therefore, for $t \geq t_w$, using the values of p, τ, θ_1, θ_2 and ϕ above:

$$
\begin{aligned}
I'_H(t) &\approx S_H(t)(c_1-\mu_H)+(1-\theta_1)V_H(t)(\alpha_4 I_A^*+\alpha_5 I_I^*+\rho_2 E^*)+(1-\theta_2)V_H(t)\rho_3 E^*+\phi V_H(t)-(\beta_H+\gamma_H+\mu_H)I_H(t)\\
&\le S_H^*(t_k^-)(c_1-\mu_H)+(1-\theta_1)V_H^*(t_k^+)(\alpha_4 I_A^*+\alpha_5 I_I^*+\rho_2 E^*)+(1-\theta_2)V_H^*(t_k^+)\rho_3 E^*+\phi V_H^*(t_k^+)-(\beta_H+\gamma_H+\mu_H)I_H(t)\\
&\le \epsilon(\beta_H+\mu_H+\gamma_H)-I_H(\beta_H+\mu_H+\gamma_H)
\end{aligned}
$$

From Lemma 2.2.1, it follows that I_H will converge to a value less than ϵ.

□

Therefore, provided that we can control all of τ, p, θ_1, θ_2 and ϕ, the infected human population can be reduced below a given threshold as $t \to \infty$. The following theorem will provide other bounds for p, τ and the infected human population under certain conditions as $t \to \infty$.

Theorem 2.2.3.
a) Let θ_1, θ_2 and ϕ be given. Then as $p \to 1$ and $\tau \to 0$, I_H will converge to $\dfrac{\pi_H}{\beta_H+\gamma_H+\mu_H}\left(\dfrac{c_2-\mu_H}{c_2}\right)$.
b) If $\theta_1=\theta_2=1$ and $\phi=0$, then for a given threshold ϵ for I_H, the minimum threshold for p is:

$$p = 1-\left[1-\frac{\pi_H}{\epsilon(\beta_H+\gamma_H+\mu_H)}\left(\frac{c_1-\mu_H}{c_1}\right)(1-e^{-c_1\tau})\right]e^{c_1\tau}.$$

c) Similarly, the minimum threshold for τ is:

$$\tau = \frac{1}{c_1} ln\left[\frac{\epsilon c_1(\beta_H+\gamma_H+\mu_H)(1-p)-\pi_H(c_1-\mu_H)}{\epsilon c_1(\beta_H+\gamma_H+\mu_H)-\pi_H(c_1-\mu_H)}\right].$$

Proof.
a) Note that at their impulsive orbits, S_H is bounded below by $S_H^*(t_k^+)$ and V_H is bounded below by $V_H^*(t_k^-)$. Therefore, for large enough t such that I_A, I_I and E are all at their equilibrium values and S_H and V_H are at their impulsive orbits:

$$
\begin{aligned}
I'_H(t) &\approx S_H(t)(c_1-\mu_H)+(1-\theta_1)V_H(t)(\alpha_4 I_A^*+\alpha_5 I_I^*+\rho_2 E^*)+(1-\theta_2)V_H(t)\rho_3 E^*+\phi V_H(t)-(\beta_H+\gamma_H+\mu_H)I_H(t)\\
&\ge S_H^*(t_k^+)(c_1-\mu_H)+V_H^*(t_k^-)\left((1-\theta_1)(\alpha_4 I_A^*+\alpha_5 I_I^*+\rho_2 E^*)+(1-\theta_2)\rho_3 E^*+\phi\right)-(\beta_H+\gamma_H+\mu_H)I_H(t)\\
&= (1-p)\,S_H^*(t_k^-)(c_1-\mu_H)+V_H^*(t_k^-)\,(c_2-\mu_H)-(\beta_H+\gamma_H+\mu_H)I_H(t)\\
&= (1-p)\,\frac{\pi_H}{c_1}\left(\frac{1-e^{-c_1\tau}}{1-(1-p)e^{-c_1\tau}}\right)(c_1-\mu_H)+S_H^*(t_k^-)\left(\frac{pe^{-c_2\tau}}{1-e^{-c_2\tau}}\right)(c_2-\mu_H)-(\beta_H+\gamma_H+\mu_H)I_H(t)\\
&= (1-p)\,\frac{\pi_H(c_1-\mu_H)}{c_1}\left(\frac{1-e^{-c_1\tau}}{1-(1-p)e^{-c_1\tau}}\right)+\frac{\pi_H}{c_1}\left(\frac{pe^{-c_2\tau}}{1-(1-p)e^{-c_1\tau}}\right)\left(\frac{1-e^{-c_1\tau}}{1-e^{-c_2\tau}}\right)(c_2-\mu_H)-(\beta_H+\gamma_H+\mu_H)I_H(t)
\end{aligned}
$$

Similarly, at their impulsive orbits, S_H is bounded above by $S_H^*(t_k^-)$ and V_H is bounded above by $V_H^*(t_k^+)$. Therefore:

$$
\begin{aligned}
I'_H(t) &\leq S^*_H(t_k^-)(c_1-\mu_H) + V^*_H(t_k^+)\,(c_2-\mu_H) - (\beta_H+\gamma_H+\mu_H)I_H(t) \\
&= \frac{\pi_H(c_1-\mu_H)}{c_1}\left(\frac{1-e^{-c_1\tau}}{1-(1-p)e^{-c_1\tau}}\right)c_1 + S^*_H(t_k^-)\left(\frac{p}{1-e^{-c_2\tau}}\right)(c_2-\mu_H) - (\beta_H+\gamma_H+\mu_H)I_H(t) \\
&= \frac{\pi_H(c_1-\mu_H)}{c_1}\left(\frac{1-e^{-c_1\tau}}{1-(1-p)e^{-c_1\tau}}\right) + \frac{\pi_H}{c_1}\left(\frac{p}{1-(1-p)e^{-c_1\tau}}\right)\left(\frac{1-e^{-c_1\tau}}{1-e^{-c_2\tau}}\right)(c_2-\mu_H) - (\beta_H+\gamma_H+\mu_H)I_H(t)
\end{aligned}
$$

Note that as $p \to 1$ and $\tau \to 0$, then $\left(\frac{1-e^{-c_1\tau}}{1-(1-p)e^{-c_1\tau}}\right) \to 0$, $\left(\frac{pe^{-c_2\tau}}{1-(1-p)e^{-c_1\tau}}\right) \to 1$ and furthermore, by l'Hopital's rule, $\left(\frac{1-e^{-c_1\tau}}{1-e^{-c_2\tau}}\right) \to \frac{c_1}{c_2}$.

Therefore, as $p \to 1$ and $\tau \to 0$, the upper bound and lower bounds of I'_H will converge to $\frac{\pi_H}{c_2}(c_2-\mu_H) - (\beta_H+\gamma_H+\mu_H)I_H(t)$. Therefore, I_H will converge to $\frac{\pi_H}{\beta_H+\gamma_H+\mu_H}\left(\frac{c_2-\mu_H}{c_2}\right)$.

Parts b) and c) of the theorem follow by noting that if $\theta_1=\theta_2=1$ and $\phi=0$, then for large t, as $I'_H(t) \approx S_H(t)(c_1-\mu_H) - (\beta_H+\gamma_H+\mu_H)I_H(t)$ and S_H is bounded above by $S^*_H(t_k^-)$, it sufficies to lower $S^*_H(t_k^-)$ below the threshold of $\frac{\epsilon(\beta_H+\gamma_H+\mu_H)}{c_1-\mu_H}$.
By Theorem 2.2.1, we note that $S^*_H(t_k^-) = \frac{\pi_H}{c_1}\left(\frac{1-e^{-c_1\tau}}{1-(1-p)e^{-c_1\tau}}\right)$. Therefore, setting $S^*_H(t_k^-) = \frac{\epsilon(\beta_H+\gamma_H+\mu_H)}{c_1-\mu_H}$:

$$
\begin{aligned}
\frac{\epsilon(\beta_H+\gamma_H+\mu_H)}{c_1-\mu_H} &= \frac{\pi_H}{c_1}\left(\frac{1-e^{-c_1\tau}}{1-(1-p)e^{-c_1\tau}}\right) \\
1-(1-p)e^{-c_1\tau} &= \frac{\pi_H}{\epsilon(\beta_H+\gamma_H+\mu_H)}\left(\frac{c_1-\mu_H}{c_1}\right)\left(1-e^{-c_1\tau}\right) \\
1-\frac{\pi_H}{\epsilon(\beta_H+\gamma_H+\mu_H)}\left(\frac{c_1-\mu_H}{c_1}\right)\left(1-e^{-c_1\tau}\right) &= (1-p)e^{-c_1\tau} \\
p &= 1-\left[1-\frac{\pi_H}{\epsilon(\beta_H+\gamma_H+\mu_H)}\left(\frac{c_1-\mu_H}{c_1}\right)\left(1-e^{-c_1\tau}\right)\right]e^{c_1\tau}
\end{aligned}
$$

Similarly, we isolate τ to obtain the other identity:

$$p = 1 - \left[1 - \frac{\pi_H}{\epsilon(\beta_H + \gamma_H + \mu_H)}\left(\frac{c_1 - \mu_H}{c_1}\right)\left(1 - e^{-c_1\tau}\right)\right] e^{c_1\tau}$$

$$1 - \frac{\pi_H}{\epsilon(\beta_H + \gamma_H + \mu_H)}\left(\frac{c_1 - \mu_H}{c_1}\right) = \left[1 - p - \frac{\pi_H}{\epsilon(\beta_H + \gamma_H + \mu_H)}\left(\frac{c_1 - \mu_H}{c_1}\right)\right] e^{-c_1\tau}$$

$$\epsilon c_1(\beta_H + \gamma_H + \mu_H) - \pi_H(c_1 - \mu_H) = \left[\epsilon c_1(\beta_H + \gamma_H + \mu_H)(1 - p) - \pi_H(c_1 - \mu_H)\right] e^{-c_1\tau}$$

$$\tau = \frac{1}{c_1} ln \left[\frac{\epsilon c_1(\beta_H + \gamma_H + \mu_H)(1 - p) - \pi_H(c_1 - \mu_H)}{\epsilon c_1(\beta_H + \gamma_H + \mu_H) - \pi_H(c_1 - \mu_H)}\right]$$

□

Note that if $\theta_1 = \theta_2 = 1$ and $\phi = 0$, then $c_2 = \mu_H$. Therefore, Theorem 2.2.3a) indicates that as $p \to 1$ and $\tau \to 0$, I_H converges to 0. Otherwise, given vaccine parameters θ_1, θ_2 and ϕ, Theorem 2.2.3a) provides a lower bound for the infected human population using pulse vaccinations.

2.3 Numerical Simulations

As known carriers of the disease, tick and rabbit populations were chosen to illustrate the ODE model presented in the paper. However, the lack of reliable records for this disease and the number of different transmission routes make it difficult to accurately estimate the transmission parameters of the ODE model. Nonetheless, using the parameter values outlined in Appendix A, we will illustrate the effects of a live vaccine on the populations of interest. These results are specific to the parameters chosen and are meant to only be illustrative; the exact scale of the effects may drastically change with different parameters.

The numerical simulations will assume that the populations are at the DFE, no other populations can be affected by the disease and at t=0, an infected tick is then introduced into the area. The human population is a rural community that has no outside contact and has approximately 1120 individuals. In order to estimate the vaccine parameters, tests indicate that when challenged, 75% of unvaccinated individuals contracted tularemia compared to 17% of individuals vaccinated with the live vaccine strain (LVS) [19]. Therefore, θ_1 was estimated to be (1 - 17/75) = 0.773. However, LVS offers 90-100% protection (average of 95% for θ_2) when challenged through other routes [19]. The capacity for reversion is unknown, so although biologically unlikely, ϕ was taken to be 0 [19].

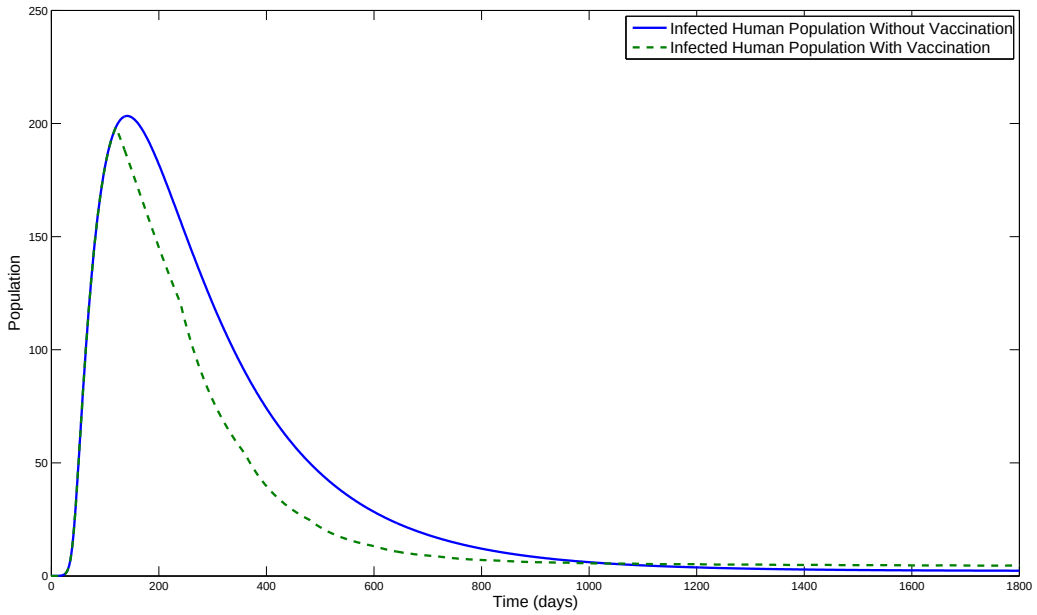

Figure 2: *Short term behaviour of the infected human population, with $p = 0.3$ and $\tau = 120$ days and the first vaccination occurring on the 120th day. All other parameter values are indicated in the text.*

Figure 2 above illustrates that an imperfect vaccine can nonetheless result in a reduction in the short-term infected human population. However, by the 1100th day, the model predicts that more people will have tularemia in the live vaccine model than in the non-vaccination model. This effect may be due to the vaccinated population which, although protected to some extent by the vaccine, may transfer more people to the infected class than the susceptible class because of its larger population. Nonetheless, in the long-run impulsive periodic orbit that is shown in Figure 3 below, the infected human population with the live vaccine is lower than without the vaccine. Figure 3 also illustrates the effects of the live vaccine on the other infected populations when compared to the model without the vaccine.

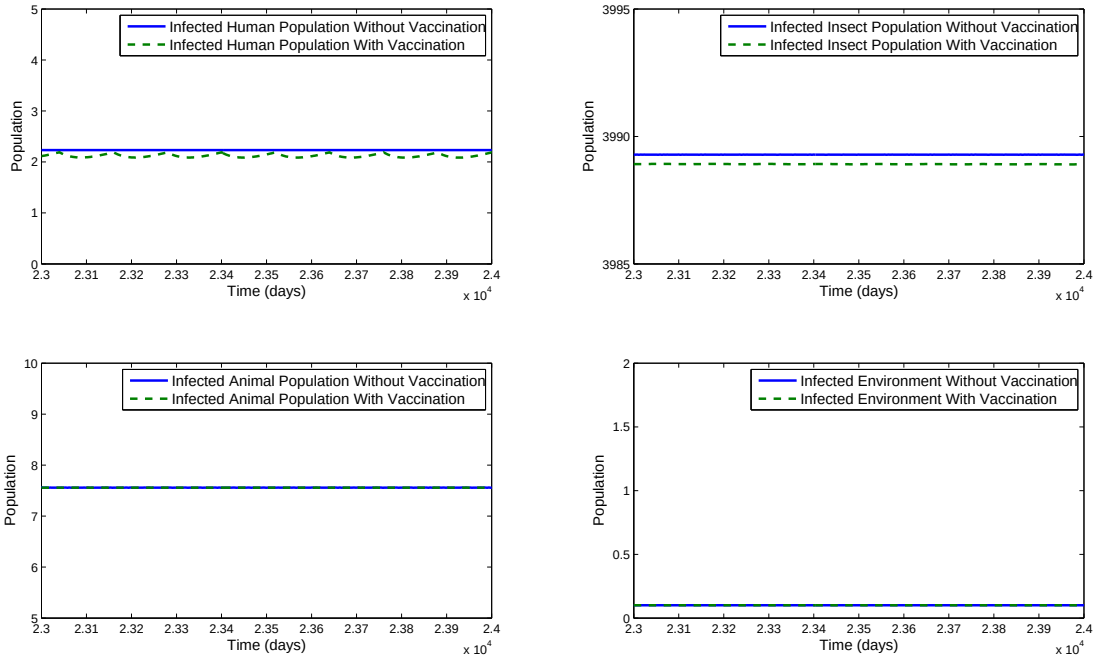

Figure 3: *Long-run behaviour of the infected populations, with $p = 0.3$, $\tau = 120$ days and the first vaccination occurring on the 120th day. All other parameter values are indicated in the text.*

The effects on the infected human population of modifying p, τ and the time before the first impulse were examined in Figure 4. While decreasing the time before the first impulse lowered the short-term infected human population, the population decreased slower to the impulsive periodic orbit than in the original case. In contrast, increasing p and decreasing τ resulted in a smaller decrease in the infected human population in the short-term, but resulted in lower long-term periodic orbits for the infected human population.

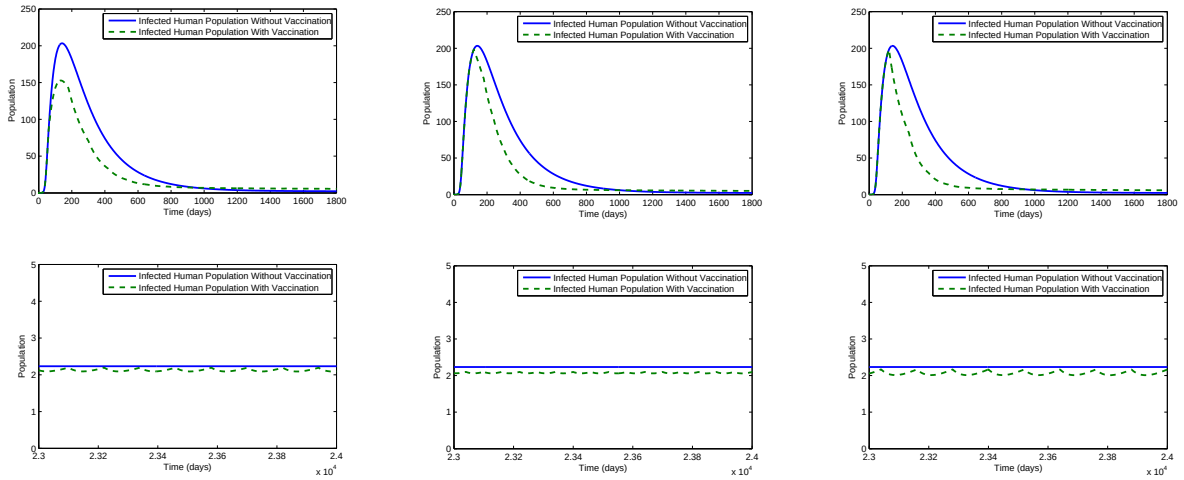

(a) p = 0.3; τ = 120 days; time to first impulse = 60 days

(b) p = 0.3; τ = 60 days; time to first impulse = 120 days

(c) p = 0.6; τ = 120 days; time to first impulse = 120 days

Figure 4: *Effects on the infected human population of changing the time before the first impulse, the time between impulses, and the proportion of people vaccinated. Short-term effects are presented in the first three graphs above, while the long-term impulses are shown below.*

We have also performed sensitivity analysis on the value of h_0 defined in Theorem 2.1.1 using Latin Hypercube Sampling for the range of values outlined in Appendix B. The results are given in Appendix C, which shows that the parameters that would have the largest effects on the system are α_1, α_2, μ_A and μ_I. Therefore, the transmission parameters - the variables that we have difficulty estimating - and the relative sizes of the human, animal and insect populations are the most crucial to the behaviour of the system.

3 Discussion

Numerical simulations illustrate that imperfect vaccines, even in the presence of an animal reservoir, can affect the outcome of an outbreak. These vaccine impulses result in a smaller infected population shortly after the first impulse, followed by a larger infected population in the medium run until it decreases to an impulsive orbit. Therefore, one of the effects of the live vaccine is to spread out the infected population over a longer period of time.

This is often desirable, as health-care centers are usually better equipped to cope with a steady stream of patients rather than a larger number of patients at one time. More time would also allow for additional resources to enter the area of concern and awareness of the risk factors to enter the community's consciousness. To this end, a variable that was shown to decrease the short-term infected human population was the time before the first vaccination impulse. Decreasing the time between vaccination impulses and increasing the proportion of susceptible humans that were vaccinated also had an effect, but the effect was not as drastic. Therefore, prompt diagnosis of the disease will be key to controlling outbreaks.

As predicted by theory, a live vaccine also has the ability to decrease the infected human population below any given threshold. However, this requires control over the vaccination parameters, which is not always possible. For example, the current LVS vaccine is imperfect and it may not be possible to force the required proportion of the susceptible population to receive the vaccine. Furthermore, the system does not specify how long it will take to reach this equilibrium, and it is possible that it decreases to the impulsive orbit so slowly that it is no longer relevant. Nonetheless, it highlights that vaccinating a large proportion of the population at regular intervals can control diseases, even when there are several different routes of transmission. Additionally, if the vaccine has perfect efficacy and no reversion rate, it provides guidelines for the proportion of susceptibles to whom the vaccine must be administered and the required frequency of the vaccinations.

In terms of cost-effectiveness, for the parameters chosen in this paper, numerical simulations indicate that a significant number of humans would be infected at the peak of the outbreak. Therefore, given the debilitating nature of tularemia, it would most likely be cost-effective to offer the vaccine for some time after the outbreak begins. However, with the relatively low number of infected humans at the impulsive orbit, it is unclear if it would be worthwhile to continue offering the vaccine indefinitely, though doing so would help control any future outbreaks. It is also important to note that the effects of the vaccine are highly dependent upon the parameters chosen - while the impulsive orbit in the simulations was lower than the equilibrium value without vaccination, this is not always the case. It might also be the case that there are few short-term effects if the vaccine cannot be administered quickly enough.

It should also be noted that this model is highly simplified. In the Northern Hemisphere, arthropods have seasonal patterns that can be accounted for and depending on the length of the outbreak, may affect the outcome of the disease. There are also several species of animals and insects that can carry the disease, all of whom interact with each other, the disease and the environment in different ways. This introduces further dynamics to the system that are difficult to model precisely and make it difficult to compare the results of the model to empirical data. Finally, all results in the numerical simulation are highly dependent upon the parameters chosen, as seen by the results of the Latin Hypercube Sampling. This analysis also shows that the crucial parameters are the ones that we had difficulty estimating. The higher the transmission rates, the smaller the window in which the first vaccination must be administered in order to have any effect. Therefore, this also emphasizes the importance of gathering accurate data and confirming assumptions before acting upon the results of any mathematical model.

4 Appendix A: Numerical Simulations

Parameter	Estimated Value	Derivation
α_1	$10^{-4} * (tick * day)^{-1}$	Estimated variable. The order of magnitude was estimated from [13], after transforming it into a daily rate and accounting for the smaller size of the rabbits.
α_2	$10^{-4} * (rabbit * day)^{-1}$	Estimated variable. The order of magnitude was estimated from [13], after transforming it into a daily rate and accounting for the smaller size of the rabbits.
α_3	$0 * (rabbit * day)^{-1}$	Rabbits do not exhibit carnivorous activity towards other rabbits.
α_4	$10^{-6} * (rabbit * day)^{-1}$	It was estimated that this rate would be approximately the same as the rate of transmission from ticks.
α_5	$10^{-6} * (tick * day)^{-1}$	It was estimated that humans would have 100 times fewer tick bites than rabbits due to lower outdoor activity, clothing and diligent removal of ticks.
α_6	$10^{-6} * (person * day)^{-1}$	It was estimated that humans would have 100 times fewer tick bites than rabbits due to lower outdoor activity, clothing and diligent removal of ticks.
α_7	$10^{-4} * environment * (rabbit * day)^{-1}$	Estimated variable. This was estimated to be the same rate as α_1.
ρ_1	$10^{-4} * (environment * day)^{-1}$	Estimated variable. This was estimated to be the same rate as α_1.
ρ_2	$10^{-4} * (environment * day)^{-1}$	Estimated variable. This was estimated to be the same rate as α_1.

Parameter	Estimated Value	Derivation
ρ_3	$10^{-4} * (environment * day)^{-1}$	Estimated variable. This was estimated to be the same rate as α_1.
β_A	$0 * day^{-1}$	We estimate that due to the susceptibility of rabbits to tularemia, they do not recover from the disease.
β_H	$1.6667 * 10^{-2} * day^{-1}$	The illness may continue for several weeks [18]. The variable was estimated at 1/60.
γ_A	$10^{-1} * day^{-1}$	Rabbits with tularemia are typically found dead. Therefore, given the susceptibility of rabbits to the disease, we estimate that the average period before death is 10 days, or the variable is approximately 1/10.
γ_H	$3.33 * 10^{-4} * day^{-1}$	The fatality rate of tularemia has been reduced to less than 2% in the United States through the use of modern antibiotics [17]. Therefore, the variable was approximated as 2% of the rate at which people are cured of the disease
π_I	$1.5224 * 10 * ticks * day^{-1}$	We estimate that the tick birth rate is approximately 20 times that of the rabbit population.
π_A	$7.6712 * 10^{-1} * rabbits * day^{-1}$	We estimate that the rabbit birth rate within the area of consideration is approximately 20 times that of the human population.
π_H	$3.8356 * 10^{-2} * people * day^{-1}$	We estimate that the average crude birth rate is 14 per 1000 people per year. Therefore, the variable was estimated at 14/365.
μ_I	$1.37 * 10^{-3} * day^{-1}$	The average life cycle of a tick is approximately 2 years [16], so the variable was estimated at 1 / (2 * 365).
μ_A	$1.191 * 10^{-3} * day^{-1}$	The average lifespan of a rabbit is 2.3 years [15], so the variable was estimated at 1/ (2.3 * 365).

Parameter	Estimated Value	Derivation
μ_H	$3.4245 * 10^{-5} * day^{-1}$	We estimate that the average lifespan is 80 years, so the variable was estimated at 1 / (80* 365).
μ_E	$7.52 * 10^{-3} * day^{-1}$	The organism can persist in water and mud for as long as 14 weeks, in straw for 6 months and in oats for 4 months [14]. An average of 133 days was chosen, so the variable was estimated at 1/133.
$S_I(0)$	π_I/μ_I	All of the state variables are taken at the disease-free equilibrium with the tick population having only a single infection.
$I_I(0)$	1	
$S_A(0)$	π_A/μ_A	
$I_A(0)$	0	
$S_H(0)$	π_H/μ_H	
$I_H(0)$	0	
$R_H(0)$	0	
$E_H(0)$	0	
$V_H(0)$	0	

5 Appendix B: Sensitivity Analysis

Variable	Start	Finish	Peak
π_I	11.568	19.28	15.424
π_A	0.57534	0.9589	0.7712
π_H	0.02740	0.04658	0.038356
α_1	0.00001	0.001	0.0001
α_2	0.00001	0.001	0.0001
α_3	0	0	0
α_4	0.0000001	0.00001	0.000001
α_5	0.0000001	0.00001	0.000001
α_6	0.0000001	0.00001	0.000001
α_7	0.00001	0.001	0.0001
ρ_1	0.00001	0.001	0.0001
ρ_2	0.00001	0.001	0.0001
ρ_3	0.00001	0.001	0.0001
β_A	0	0.005	0
β_H	0.01282	0.02381	0.016667
γ_A	0.05	0.15	0.1
γ_H	0.0001667	0.000666	0.000333
μ_I	0.00068493	0.002740	0.001370
μ_A	0.00054794	0.001370	0.001191
μ_H	0.0000332232	0.0000391389	0.000034245
μ_E	0.0055556	0.0102	0.00752

6 Appendix C: Results of Latin Hypercube Sampling

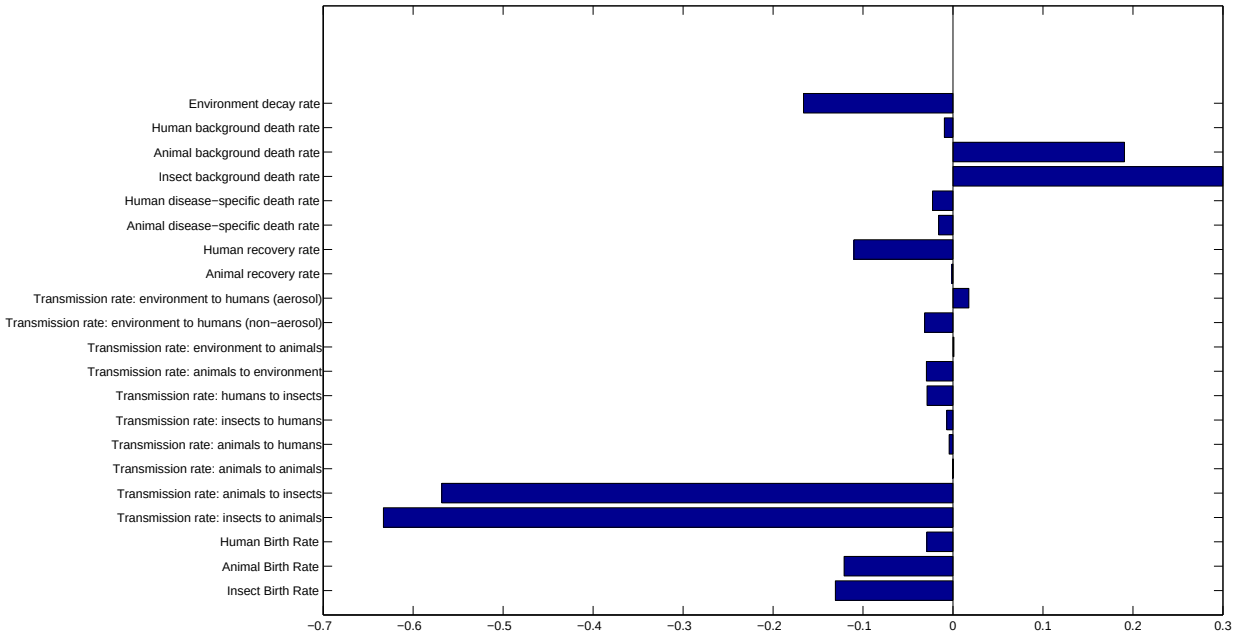

Figure 5: *Results of parameter sensitivity analysis using Latin Hypercube Sampling.*

7 Bibliography

[1] Edward B. Hayes. Looking the other way: Preventing vector-borne disease among travelers to the United States. Travel Medicine and Infectious Disease, 8: 277-284, 2010.

[2] Petra C.F. Oyston and Janine E. Quarry. Tularemia vaccine: past, present and future. Antonie van Leeuwenhoek, 87: 277-281, 2005.

[3] Karen L. Elkins, Siobhn C. Cowley, Catharine M. Bosio. Innate and adaptive immune responses to an intracellular bacterium, Francisella tularensis live vaccine strain. Microbes and Infection, 5, 135-142.

[4] Janet E. Foley and Nathan C. Nieto. Tularemia. Veterinary Microbiology, 140: 332-338, 2010.

[5] A Sjstedt. Tularemia: history, epidemiology, pathogen physiology, and clinical manifestations. Annals of the New York Academy of Sciences, 1105:1-29, 2007

[6] Michael Green, Glyn Choules, Debbie Rogers and Richard W. Titball. Efficacy of the live-attenuated Francisella tularensis vaccine (LVS) in a murine model of disease. Vaccine, 23(20): 2680-2686, 2005.

[7] Petra C.F. Oyston, Anders Sjstedt and Richard W. Titball. Tularemia: bioterrorism defence renews interest in Francisella tularensis. Nature Review Microbiology, 2(12): 967-979, 2004.

[8] Hakan Leblebicioglu, Saban Esen, Derya Turan, Yucel Tanyeri, Guher Goral, Fatma Ziyagil, Aynur Karadenizli. Outbreak of tularemia: a case " control study and environmental investigation in Turkey. International Journal of Infectious Diseases, 12: 265-269, 2008.

[9] Anders Johansson, Mats Forsman, and Anders Sjstedt. The development of tools for diagnosis of tularemia and typing of Fancisella tularensis. APMIS, 112: 898-907, 2004.

[10] E Nonaka, GD Ebel, HJ Wearing. Persistence of Pathogens with Short Infectious Periods in Seasonal Tick Populations: The Relative Importance of Three Transmission Routes. PLoS ONE 5(7): e11745. doi:10.1371/journal.pone.0011745, 2010.

[13] Holly Gaff and Louis Gross. Modeling Tick-Borne Disease: A Metapopulation Model. Bulletin of Mathematical Biology, 69: 265-288, 2007.

[14] Katerine Feldman, Russell Enscore, Sarah Lathrop, Bela Matyas, Michael McGuil, Martin

Schriefer, Donna Siles-Enos, David Dennis, Lyle Petersen and Edward Hayes. An Outbreak of Primary Pneumonic Tularemia on Marthas Vineyard. The New England Journal of Medicine, 345: 1601-1606, 2001.

[15] Heiko Rodel, Agnes Bora, Jurgen Kaiser, Paul Kaetzke, Martin Khaschei and Dietrich Von Holst. Density-dependent reproduction in the European rabbit: a consequence of individual response and age-dependent reproductive performance. Oikos, 104: 529-539, 2004.

[16] Vapalahti Lindquist. Tick-borne encephalitis. The Lancet, 371: 1861-1871, 2008.

[17] Anders Sjostedt. Tularemia: History, Epidemiology, Pathogen Physiology, and Clinical Manifestations. Annals of New York Academic Science, 1105: 1-29, 2007.

[18] Tularemia. www.ncbi.nlm.nih/gov/pubmedhealth/PMH0001859. Accessed April 4, 2011. PubMed Health. Last reviewed March 17, 2009.

[19] J. Conlan and Petra Oyston. Vaccines against Francisca tularensis. Annals of New York Academic Science, 1105: 325-350, 2007.

[20] J.M. Petersen, P.S. Mead, M.E. Schriefer. Francisella tularansis: an arthropod-borne pathogen. Vet. Res., 40:07. DOI: 10.1051/vetres:2008045, 2009.

[21] Tularemia. $http://www.cdc.gov/tularemia/Surveillance/Tul_{C}asesbyState.html$. Accessed March 2, 2011. CDC. Last reviewed December 21, 2009.